Int. J. Chem. Sci.: 12(4), 2014, 1527-1537
ISSN 0972-768X
www.sadgurupublications.com

KINETIC AND MECHANISTIC STUDY OF THE OXIDATION OF ORANGE-II BY HEXACYANOFERRATE (III) IONS CATALYZED BY IRIDIUM NANOCLUSTERS

ANJALI GOEL*, RANJANA BHATT and RAJNI LASYAL

Department of Chemistry, Kanya Gurukul Campus, Gurukul Kangri University,
HARDWAR (U.K.) INDIA

ABSTRACT

Since aromatic azo-dyes-widely used for dyeing textiles – are toxic and potential carcinogens. It is essential to develop methods for their degradation in textile industry wastewater for letting this water out. In the present study, results of the degradation of orange-II, an azo-dye, through oxidation by potassium hexacyanoferrate ions catalyzed by Iridium-nanoclusters are presented.

The kinetics of the reaction has been studied spectrophotometrically at 484 nm, the λ_{max} of the dye. The kinetics obeys the rate law:

$$R_{obs} = k_3\,[HCF][dye]\,[catalyst][OH^-]$$

where R_{obs} is the initial rate, k_3 is the rate constant and [HCF], [dye], [catalyst] and $[OH^-]$ represent the concentrations of reagents in parenthesis. The energy of the activation was found to be 9.6 Kcal mol^{-1}. A reaction mechanism, which assumes the formation of a transient complex between Ir-nano and anionic form of the dye has been suggested. The products have also been analyzed.

Key words: Iridium, Nanoparticles, Hexcyanoferrate, Orange-II azo dye, Oxidation, Catalysis.

INTRODUCTION

The emergence of diverse classes of synthetic dyes including azo-dye occurred due to constant effort to find specific dye for a particular class of application on diverse materials of industrial importance mainly textile fibres, aluminium sheet, leather, electro optical devices, ink-jet printers etc.[1-3] Dyes released from the textile, paper, printing, pharmaceutical and food industries pollute the water[4-5]. Thus, it is very essential to degrade dyes and make the enviornment free of toxicity. Usually complete demineralisation is expensive with physico-chemical methods[6]. In the past few years, nanoparticles have been

---

*Author for correspondence; E-mail: anjaligoel10@gmail.com

used for the degradation of several dyes. Recently, for dye wastewater treatment, a few reports have been published using nanoscale zero valent iron (nZVI) to remove azo dyes, methyl orange and basic yellow 28[7,8]. Noble metal nanoparticles with high specific catalytic activity are ubiquitous in modern synthetic organic chemistry during the recent decades[9]. In this study, colloidal dispersion of iridium nanoclusters synthesized by wet reduction method[10,11] has been used as catalyst to oxidize orange-II, an azo dye, by potassium hexacyanoferrate (III) (HCF) in aqueous alkaline media. The nano particles displayed a much better catalytic activity than the molecular iridium.

EXPERIMENTAL

Reagents and chemicals

All the chemicals and reagents used were of AR grade. Azo dye used was orange –II (Sigma Aldrich) and its structure is:

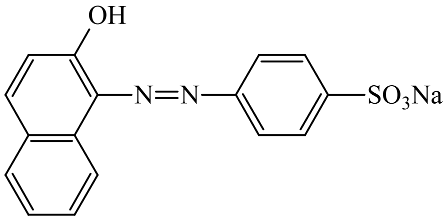

All solutions were prepared in doubly distilled water. HCF was recrystallized before use. Its stock solutions was kept in amber coloured bottle to prevent its photodecomposition. Merck make potassium chloride and sodium hydroxide were used for maintaining the desired ionic strength and alkalinity, respectively. The iridium trichloride, $IrCl_3.3H_2O$, used was of Merck.

To prepare iridium nano dispersion, calculated amount of $IrCl_3.3H_2O$ and polyvinylpyrrolidone (protecting agent, mean molecular weight 40,000) were dissolved in methanol/water mixed solvent (5/4.6, v/v) to make their final concentration 7.07×10^{-4} M and 8.69×10^{-5} M, respectively. Thereafter, 1 mL of 0.2 M NaOH was added dropwise with continuous stirring. The reaction mixture so obtained was refluxed for 1.5 hr to obtain irdium nano-clusters in suspension. The particle size of iridium nanocluster was determined using XRD and TEM methods of analysis as reported earlier[12].

Kinetics measurements

The kinetics was studied as follows. The required quantities of standard solutions of HCF, NaOH, KCl, iridium nano-particles were taken in a flask and sufficient water was added to make 100 mL reaction mixture. The reaction mixture and stock solution of dye were then equilibriated separately in a thermostat at 40 ± 0.1^{o}C. To initiate the reaction, a required amount of dye solution was added to the mixture.

Aliquots were withdrawn from the reaction mixture periodically, and the progress of the reaction was followed spectrophotometrically by measuring the absorbance at 484 nm, which is λ_{max} of orange-II.

Initial rates, $(d[dye]/dt)_i$ were evaluated using plane mirror method from the plots of absorbance, A, versus time, t. The first order rate constant was calculated by plot of log A_t versus t. For obtaining best-fit curves, the least squares method was used in each case. The replicate rate measurements were reproducible within ± 10%.

Product analysis/UV-Vis and FT-IR spectral studies

Product analysis and decolourization was monitored by UV-Vis spectroscopy (Figure 1). Decolourization of dye was followed by monitoring the changes in its absorption spectrum (200-700 nm) using a Systronic-117 UV-Vis spectrophotometer under the same experimental conditions, which were used for the kinetic study. The disappearance of peak at 484 nm in UV-Vis spectra show the degradation of orange-II by HCF (III). Appearance of a new peak at 222 nm suggests the formation of a new product. For FT-IR studies, the solution of substrate, oxidant and NaOH (ionic strength is adjusted by the requisite amount of KCl), were mixed and kept at atmospheric conditions for 24 hrs. The product was extracted with ethyl acetate and identified by FT-IR spectroscopy. The result of FT-IR spectra are presented in Figure 2.

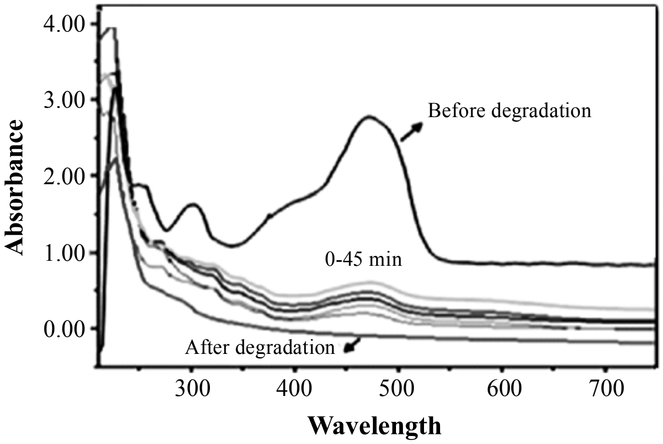

Fig. 1: UV-Vis spectra during decolorization of orange-II

The comparison of FTIR of control dye orange-II and extracted product Fig. 2 (a & b) indicates the oxidation of the parent dye compound. It is well known that the peaks at 1620, 1508, 1460 cm^{-1} of azo dye were assigned to –C=C– stretching of benzene ring, naphthalene ring stretching and–N=N- stretching of dye, respectively. Furthermore the peaks at 1056 and 1280 cm^{-1} were assigned to SO_3H stretching of benzene sulphonic acid and the peak at 1122 cm^{-1} were assigned to –OH stretching and deformation of hydroxybenzene[13].

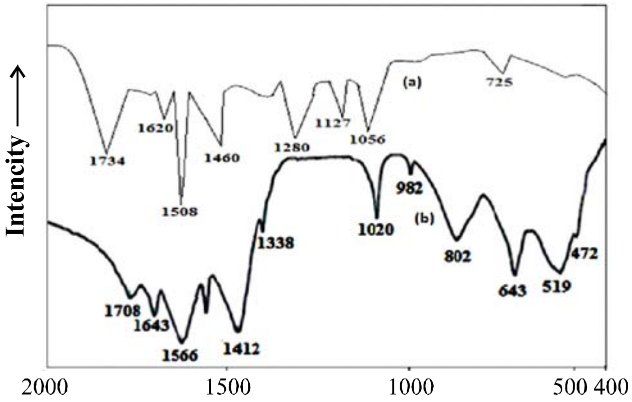

Fig. 2: FT-IR spectra of orange-II (a) before and (b) after oxidation

The FT-IR spectra of extracted product showed a significant change in the band positions compared to control dye spectrum. The disappearance of bands near 725, 1127 and 1280 and formation of new bands shows the degradation of azo dye into some simple product. Bands at 1708 and 1643 cm^{-1} indicates the presence of aryl acid and new bands at 1566 cm$^{−1}$ and 1412 cm$^{−1}$ pointed towards the N-H bending and C-N stretching, respectively.

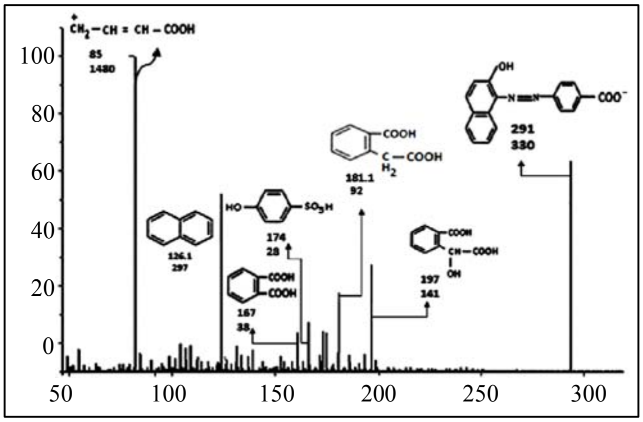

Fig. 3: LC-MS spectra of fragmentation products of orange-II

Products of orange-II oxidation were also analyzed by LC-MS (Q-t- of Mcromass). Based on mass spectra, seven compounds are identified after the oxidation of orange-II, which are small, less hazardous molecules with low molecular weight of (m/z) values at 291, 197, 174, 167, 181, 126 and 85. The possible structures of fragmentation products are shown in Figure 3[14,15].

RESULTS AND DISCUSSION

Preliminary investigations

The entire kinetics work has been done in aqueous alkaline medium. In the series of kinetics runs, the experimental conditions set were as follow: [HCF] = (1-9) × 10^{-6}, [Orange-II] = (2 – 8) × 10^{-5}, [OH^-] =0.25, [Ir nano] = 6.15 × 10^{-7} and I = 0.3 mol dm^{-3}. The size of iridium nano-particles used as catalyst was 4.5 ± 0.4 nm. The preliminary investigations carried out in the presence of Ir precursor and Ir nano as catalyst showed the reaction to be faster in the presence of Ir nano than Ir precursor (Figure 4).

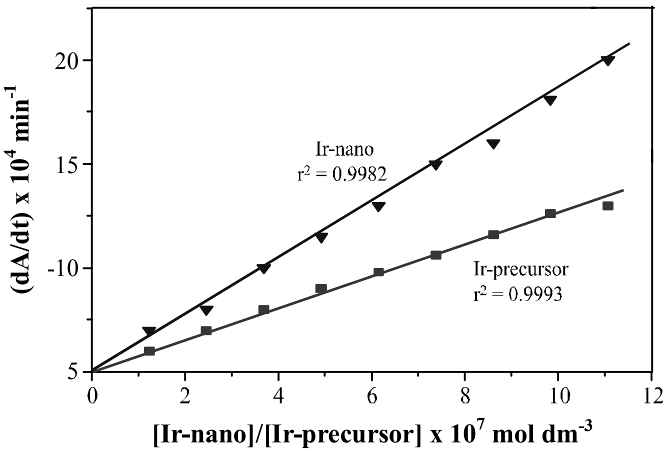

Fig. 4: Rate of oxidation of orange-II by Ir-nano and Ir-Precursor

Since the kinetics has been studied by following the decrease in the concentration of the reagent in excess, so the treatment of the kinetics is based on the determination of the initial rates, R_{obs}. The R_{obs} values were determined from the plots of *A* versus *t*. The R_{obs} values given in Table 1 clearly show first order in each of [HCF], [dye] and [catalyst] as defined by the rate law:

$$R_{obs} = k_2[HCF][Dye][Catalyst] \quad ...(1)$$

The rate increased linearly on increasing $[OH^-]$ as shown in Table 1, which indicates a first order in $[OH^-]$ also. On including $[OH^-]$ dependence the rate law (1) modifies to Eq. (2).

$$R_{obs} = k_3 [HCF][Dye] [Catalyst][OH^-] \quad \ldots(2)$$

where $k_2 = k_3 [OH^-]$

An increase in ionic strength with the help of KCl led to an increase in rate (Table1).

Table 1: Effect of different reactants concentration on reaction rate at 40 ± 0.1°C at λ_{max} 484 nm and [Ir nano] = 6.15×10^{-7} mol dm^{-3}

$[O\text{-}II] \times 10^{-5}$ mol dm^{-3}	$[OH]^-$ mol dm^{-3}	HCF (III) $\times 10^{-6}$ mol dm^{-3}	I mol dm^{-3}	R_{obs} 10^{-4} min^{-1}
2.0	0.25	3.0	0.3	6.8
3.0	0.25	3.0	0.3	9.5
4.0	0.25	3.0	0.3	13.0
5.0	0.25	3.0	0.3	16.0
6.0	0.25	3.0	0.3	19.0
7.0	0.25	3.0	0.3	22.0
8.0	0.25	3.0	0.3	26.0
3.0	0.10	3.0	0.3	3.0
3.0	0.15	3.0	0.3	6.0
3.0	0.20	3.0	0.3	9.0
3.0	0.25	3.0	0.3	13.3
3.0	0.25	1.0	0.3	4.4
3.0	0.25	2.0	0.3	6.8
3.0	0.25	3.0	0.3	11.0
3.0	0.25	4.0	0.3	14.0
3.0	0.25	5.0	0.3	17.0
3.0	0.25	6.0	0.3	21.0

Cont…

$[O\text{-}II] \times 10^{-5}$ mol dm^{-3}	$[OH]^{-}$ mol dm^{-3}	HCF (III) × 10^{-6} mol dm^{-3}	I mol dm^{-3}	$R_{obs}\ 10^{-4}$ min^{-1}
3.0	0.25	7.0	0.3	24.0
3.0	0.25	8.0	0.3	27.0
3.0	0.25	9.0	0.3	30.0
3.0	0.25	3.0	0.3	20.0
3.0	0.25	3.0	0.35	26.0
3.0	0.25	3.0	0.40	33.0
3.0	0.25	3.0	0.45	40.0
3.0	0.25	3.0	0.5	45.0

Effect of temperature

The effect of temperature on the reaction kinetics of orange-II with HCF (III) was investigated over the temperature range of 40 to 55°C under pseudo first order conditions, which indicates that azo-dye degradation efficiency increases with increasing temperature. Activation parameters were evaluated from linear Arrhenius plots. The values of energy of activation (E_a), enthalpy of activation (ΔH), entropy of activation (ΔH) evaluated are given in Table 2.

Table 2: Activation parameters at [HCF (III)] = 3×10^{-6} M, [Dye] = 3×10^{-5} M, $[OH^{-}]$ = 0.25 M, I = 0.3 M

E_a Kcal mol^{-1}	10^6A L mol^{-1} s^{-1}	$-\Delta S^{\#}$ e. u.	$\Delta H^{\#}$ Kcal mol^{-1}	$\Delta G^{\#}$ Kcal mol^{-1}
9.60	6.97	29.25	8.80	18.18

A first order in each of [Dye], [HCF], [Catalyst] and $[OH^{-}]$ indicates the operation of a multistep mechanism. Since HCF is known not to show any acid-base reaction with OH^{-} ion, the latter appears to react with dye extract a proton and form an anionic species, D^{-}, in an equilibrium. It appears reasonable to assume the formation an intermediate, C, between D^{-} and the catalyst nano- Ir particles, Ir_n, rather than between two negatively charged species, D^{-} and $Fe(CN)_6^{3-}$.

Based on the above discussion and the experimental rate law, and previously reported work,[16,17] the following reaction mechanism for the oxidation of dye may be proposed.

$$\text{(I)}\qquad D + OH^- \underset{}{\overset{K}{\rightleftharpoons}} D^- + H_2O$$

$$\text{(II)}\qquad D^- + Ir_n \underset{k_{-1}}{\overset{k_1}{\rightleftharpoons}} \text{Complex (C)}$$

$$\text{(III)}\qquad C + Fe(CN)_6^{3-} \xrightarrow[\text{Slow}]{k_2} Ir_n + Fe(CN)_6^{4-} + IP$$

$$\text{(IV)}\qquad IP \xrightarrow{[O]} Pr$$

Scheme 1

In **Scheme 1**, it is assumed the equilibria (I) and (II) are rapidly established. A clean-cut first order in each of [Dye], [Ir-nano-cluster] and [OH^{-1}] indicates the equilibria (I) and (II) to be fast and the values of equilibrium constants, K and K_1 to be quite low. The reaction of the intermediate, C, with HCF is assumed to be slow yielding another intermediate, IP, probably a very reactive radical species, owing to 1-electron oxidation of dye by $Fe(CN)_6^{3-}$. The catalytic species Ir_n is regenerated. Subsequently the intermediate, IP, is oxidized by HCF in one or more rapid steps to yield final products.

Since, step (III) is rate-determining, the rate of the reaction is given by Eq. (3).

$$R_{obs} = k\,[C]\,[HCF] \qquad \text{…(3)}$$

From Equilibria (III) and (IV) we get,

$$[D^-] = K\,[D]\,[OH^-] \qquad \text{…(4)}$$

and

$$[C] = K_1\,[D^-]\,[Ir_n] \qquad \text{…(5)}$$

Where $K_1 = k_1 / k_{-1}$

On substituting the value of [D^-] from Eq. (4) into Eq. (5), we get derived rate law as Eq. (6),

$$R_{obs} = kKK_1\,[D]\,[Ir_n]\,[HCF]\,[OH^-] \qquad \text{…(6)}$$

which as same as experimental rate law (2) through $k_3 = kKK_1$.

On the basis of above mechanism and mass spectrometric results, the following oxidation pathway is proposed (**Scheme 2**).

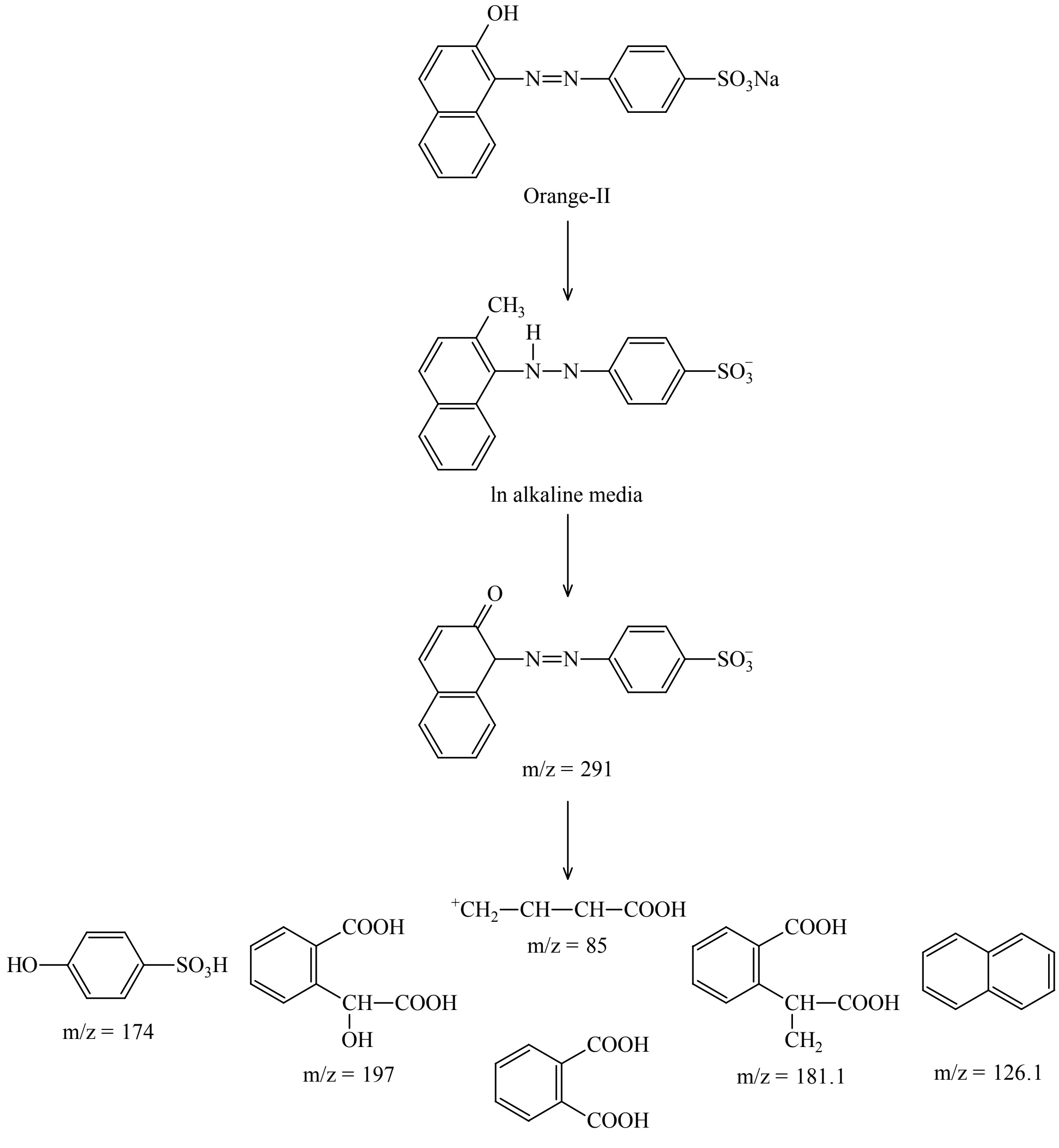

Low molecular weight products

Scheme 2: Oxidation pathway of Orange-II

CONCLUSION

The kinetics study on nano catalysis shows iridium(0) nano-particles to act as better catalyst than the Ir(III) ions. In strong alkaline medium, azo dye, orange-II, is degraded into some simple low molecular weight products. Therefore, this reaction offers an opportunity of converting in to a technology for degradation from complex organic molecule into simpler non-toxic molecules and helping in making the environment green.

REFERENCES

1. H. Zollinger, Dyes and Pigments, VCH Publishers, New York (1987) p. 92.
2. C. W. Maynard, Riegel's Handbook of Industrial Chemistry, 3rd Ed. Van Nostard Reinhold, New York (1983) p. 809.
3. S. C. Catino and R. E. Farris, Concise Encyclopedia of Chemical Technology, M. Grayson Ed., John Wiley & Sons, New York (1985) p. 142.
4. E. Adamek, W. Baran, J. Ziemianska and A. Sobczak, Int. J. Photoenergy, Article ID 578191, 1 (2013).
5. K. Dutta, S. Bhattacharjee, B. Chaudhuri and S. Mukhopadhyay, J. Environ. Sci. and Health, Part A- Toxic/Hazardous Substances and Environmental Engineering, **38(7)**, 1311 (2007).
6. R. Byberg, J. Cobb, L. D. Martin, R. W. Thompson, T. A. Camesano, O. Zahraa and M. N. Pons, Enviorn. Sci. Pollut. Res., **20**, 3570 (2013).
7. S. A. Singh and G. Madras, Seperation and Purification Technology, **105**, 79 (2013).
8. Y. H. Shih, C. P. Tso and L. Y. Tung, J. Environ. Eng. Manage., **20(3)**, 137 (2010).
9. T. Poursaberi, M. Hassanisadi and F. Nourmohammadian, Prog. Color Colorants Coat., **5**, 35 (2012).
10. S. Jansat, M. Gomez, K. Philippot, G. Muller, E. Guiu, C. Claver, S. Castillon and B. Chaudret, J. Am. Chem. Soc., **126**, 1592 (2004).
11. M. Faraday, Philos. Trans. R. Soc. London, **147**, 145 (1857).
12. A. Goel, R. Bhatt, Neetu, Int. J. Res. Chem. Environ., **2(1)**, 210 (2012).
13. E. Ember, S. Rothbar, R. Puchta and R. Eldik, New J. Chem., **33(1)**, 34 (2009).
14. J. X. Chen and L. Zhu, International Conference on Advances in Energy Engineering, 281 (2010).

15. A. Stolz, Appl. Microbiol. Biotechnol., **56**, 69 (2001).

16. V. Vatanpour, N. Daneshvar and Mohd H. Rasoulifard, J. Environ. Eng. Manage., **19(5)**, 277 (2009).

17. K. S. Gupta and Y. K. Gupta, J. Chem. Edu., **61**, 972 (1984).

Revised : 21.09.2014 *Accepted : 24.09.2014*